JAM CM Journal of Applied Mathematics and Computational Mechanics 2025, 24(3), 98-107
www.amcm.pcz.pl p-ISSN 2299-9965
DOI: 10.17512/jamcm.2025.3.06 e-ISSN 2353-0588

THERMOPLASTIC INJECTION MOLDING PROCESS SIMULATIONS AND THEIR EXPERIMENTAL VERIFICATION

Jacek Nabiałek, Dariusz Kwiatkowski

Department of Technology and Automation, Czestochowa University of Technology
Częstochowa, Poland
jacek.nabialek@pcz.pl, dariusz.kwiatkowski@pcz.pl

Received: 21 June 2025; Accepted: 19 August 2025

Abstract. The simulation of the thermoplastic injection process was carried out using the Autodesk Simulation Moldflow Insight software. The seven-parameter Cross-WLF rheological model was adopted for the tests. Knowledge of the pvT relationship is essential for simulating the pressing phase and for determining the residual stresses and deformation of the molded parts. For this purpose, the Tait equation was used in the numerical analysis. In the initial stage of the simulation, a solid model of the molded part was created using the Siemens NX software. In the subsequent step, the molded part model was imported, and the FEM mesh was applied. Then, the injection process parameters were entered into the program. This data included thermal, rheological, and mechanical properties of the injected thermoplastic. The recorded video sequences were compared with the results of numerical simulations, and the extent to which computer modeling of the injection process can be useful in practice was assessed.

MSC 2010: *74S05, 76A10*
Keywords: *simulations, injection molding, thermoplastics*

1. Introduction

Polymer processing using the injection molding method is a widely used technology across many sectors of modern industry. This method is applied in the production of packaging, structural moldings, household appliances, electronic equipment components, automotive parts, and many other products. Given its extensive applications, conducting scientific research aimed at a thorough understanding of the phenomena occurring during mold filling can contribute to a more effective tool design and reduction in both implementation and production time. The papers [1-5] present selected results of polymer flow tests during filling of the injection mold cavity.

This study attempts to present selected results of research focused on computer modeling of polymer flow within the mold cavity during the filling phase. The results of computer simulations are compared with recorded observations of polymer flow

during injection. Similar studies are conducted by various scientific institutions worldwide [6-10]. To the best of the authors' knowledge, no similar research is currently being conducted at the national level.

2. Fundamentals and assumptions

The fundamental equations that need to be solved are [11-14]:

- The mass conservation equation,
- The momentum conservation equation,
- The energy conservation equation.

$$\frac{\partial \rho}{\partial t} + \frac{\partial}{\partial x_i}(\rho v_i) = 0 \tag{1}$$

$$\rho\left(\frac{\partial v_j}{\partial t} + v_i \frac{\partial v_j}{\partial x_i}\right) = -\frac{\partial p}{\partial x_j} + \frac{\partial \tau_{ij}}{\partial x_i} + \rho g_i \tag{2}$$

$$\rho c_p\left(\frac{\partial T}{\partial t} + v_i \frac{\partial T}{\partial x_i}\right) = k\frac{\partial^2 T}{\partial x_i^2} + \tau_{ij}\frac{\partial v_j}{\partial x_i} \tag{3}$$

where:

ρ – density,
t – time,
v_i – velocity components,
p – pressure,
τ_{ij} – shear stress components,
T – temperature,
c_p – specific heat,
g_i – gravity force components.

These equations, in their general form, cannot be directly solved for a process as complex as injection molding. Therefore, several simplifying assumptions must be made. These assumptions concern both the properties of the polymer and the shape of the region where the equations are applied. A key simplifying assumption is the introduction of the concept of the no-flow temperature – the temperature below which the polymer can be considered to behave as a solid.

By assuming the no-flow temperature, the velocity components of the solidified polymer at the mold cavity walls are considered to be zero. Additionally, it is assumed that the polymer flow is symmetric with respect to the mid-plane of the molding cavity. Equations (1), (2), and (3) are solved separately for the mold filling packing phases under the following boundary conditions:

- Pressure is zero at points located on the flow front,
- A specified pressure or flow rate is applied at the polymer injection point(s),

- The pressure gradient in the normal direction is zero at the boundary points of the molding cavity,
- The temperature of the molding cavity walls or specified points of the injection mold walls is defined,
- The temperature gradient along the z-axis at the mid-plane of the molding cavity is zero,
- The temperature of the molten polymer at the injection point(s) is specified.

To conduct a simulation of the injection molding process, it is necessary to determine viscosity curves for the selected polymer material. A viscosity curve represents the relationship between the material's viscosity and the shear rate, as defined by the selected rheological model. Several well-known models are used for this purpose. When choosing a rheological model, attention should be paid to the accuracy of the representation and the availability of data for its determination.

The most commonly used rheological models are [15-17]:

- Power-law model,
- Moldflow second-order model (logarithmic model),
- Cross-WLF model,
- Carreau model.

Below is the mathematical interpretation of the rheological models most frequently used in polymer injection molding simulations.

➢ Power law model

The mathematical description of the power-law model is given by [15]:

$$\eta = m\,\dot{\gamma}^{n-1} \tag{4}$$

where η is viscosity, $\dot{\gamma}$ is the shear rate, m is the flow consistency index, and n is the power law index (flow behavior index).

For polymer blends, the power law index n has a value in the range of 0.2 to 0.8. Taking the logarithm of both sides of equation (4) yields:

$$\ln(\eta) = (n-1)\ln(\dot{\gamma}) + \ln(m) \tag{5}$$

The relationship between $\ln(\eta)$ and $\ln(\dot{\gamma})$ is linear. For this reason, the power-law model effectively describes polymer behavior in the high shear rate region. This model can also be relatively easily fitted to experimental data, allowing for the determination of the rheological parameters m and n.

The main drawback of the power-law model is its poor representation in the low shear rate range. Despite this limitation, it is widely used for modeling flow in injection molding. In particular, during the filling phase, shear rates are often sufficiently high to justify the use of the power-law model.

The dependence on temperature is typically introduced by multiplying equation (4) by an exponential term [15]:

$$\eta = m\,\dot{\gamma}^{n-1}\exp(c\,T) \tag{6}$$

where c is a constant and T is the temperature. The power-law model in the form of (4) is referred to as the first-order viscosity model, available in flow simulation software.

- Moldflow second-order model (logarithmic model)

To improve viscosity modeling at low shear rates, the following rheological model is used [15]:

$$\ln\eta = A_0 + A_1\ln\dot{\gamma} + A_2T + A_3(\ln\dot{\gamma})^2 + A_4T\ln\dot{\gamma} + A_5T^2 \tag{7}$$

where A_i are constants.

This model raises concerns because it is based on empirical observations. However, this has little significance in the context of the issues discussed in this study. The goal is to find a model that fits the experimental data as closely as possible, and the second-order model is capable of characterizing the observed behavior of polymers in a plastic state.

There are certain limitations to this model. The most important one is that, although it is highly flexible, the model may suggest behavior that is not rheologically reasonable. For example, it is possible [2] that $\delta\eta/\delta\dot{\gamma} > 0$, implying that viscosity increases with shear rate, which is clearly unrealistic.

- Cross-WLF model

The mathematical form of the Cross-WLF model is given as [16]:

$$\eta(\dot{\gamma},T,p) = \frac{\eta_0(T,p)}{1+\left(\frac{\eta_0\dot{\gamma}}{\tau^*}\right)^{1-n}} \tag{8}$$

The Williams-Landel-Ferry (WLF) equation is an empirical equation used to describe the dependence of viscosity η_0 on temperature T and pressure p. It is expressed as follows:

$$\eta_0(T,p) = D_1\cdot\exp\left[-\frac{A_1(T-T^*)}{A_2+(T-T^*)}\right] \tag{9}$$

with

$$T^*(p) = D_2 + D_3\cdot p \tag{10}$$

$$A_2 = \tilde{A}_2 + D_3\cdot p \tag{11}$$

where:
T – temperature,
p – pressure,

n, τ^* – constant parameters of the Cross-WLF model (τ represents the shear stress at which the polymer in the liquid state exhibits shear-thinning behavior),
η_0 – viscosity at a shear rate approaching zero,
D_1, D_2, D_3, A_1 – constant parameters of the WLF equation.

In numerical calculations, the Tait equation was used to represent changes in specific volume $\vartheta(p,T)$ along an isotherm, based on two variable parameters, C and B, which are functions of temperature. It is most commonly expressed in the following form [18]:

$$\vartheta(p,T) = \vartheta_0(T) \cdot \left\{1 - C \cdot ln\left[1 + \frac{p}{B(T)}\right]\right\} + \vartheta_t(p,T) \tag{12}$$

where:

for $T > T_m$
$$\vartheta_0(T) = b_{1m} + b_{2m}(T - b_5) \tag{13}$$

for $T < T_m$
$$B(T) = b_{3m} \cdot \exp[-b_{4m} \cdot (T - b_5)] \tag{14}$$

$$\vartheta_0(T) = b_{1s} + b_{2s}(T - b_5) \tag{15}$$

$$B(T) = b_{3s} \cdot \exp[-b_{4s} \cdot (T - b_5)] \tag{16}$$

where:
$\vartheta_0(T)$ – specific volume at atmospheric pressure,
T – temperature,
T_m – melting temperature,
p – pressure,
C – universal constant (0.0894).

This applies to semi-crystalline materials $\vartheta_T(p,T) = b_7 \cdot \exp[b_8 \cdot (T - b_5) - b_9 \cdot p]$.

- Carreau model

The Carreau model is mathematically expressed as follows [8]:

$$\frac{\eta - \eta_\infty}{\eta_0 - \eta_\infty} = [1 + (\lambda \cdot \dot{y})^2]^{(n-1)/2} \tag{17}$$

where η_∞ is the viscosity at infinite shear rate, η_0 is the viscosity at zero shear rate, n is a constant with the same interpretation as in equation (4), and λ is the time constant.

3. Research methodology

This study presents the results obtained from an investigation of a PBT/PET composite with glass fiber reinforcement. The material used was CELANEX 2302 GV1/15, a product of TICONA EUROPE, with a glass fiber content of 15 % by weight. The melt volume-flow rate (MFR) of the material is 20 cm^3/10 min (measured at

265 °C under a load of 2.16 kg), and its density is 1.43 g/cm^3. This polymer blend introduced several technological challenges, primarily due to the specific processing characteristics of the PBT/PET system. These included difficulties in ejecting the molded part from the mold, solidified material sticking in the gate area, and material leakage from the plasticizing unit.

The processing equipment used in the study was an Engel injection molding machine (Victory 200/50 spex), equipped with a high-quality control system. The use of a high-precision modern machine allowed for the resolution of all the aforementioned issues.

As part of the simulation studies, a series of numerical analyses were conducted to computationally model the injection molding process. For this purpose, the professional simulation software Moldflow Plastics Insight (version 2019) was used. To ensure accurate analyses, material data had to be input. This was done using the database integrated into the simulation program.

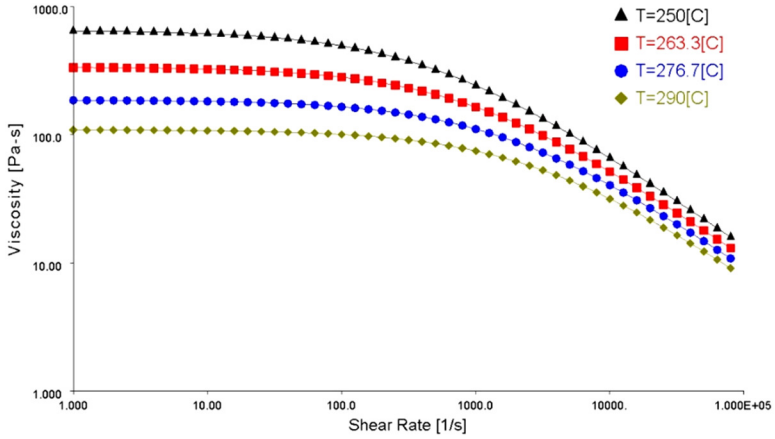

Fig. 1. Viscosity curves of PBT/PET 15GF (Moldflow Materials Database)

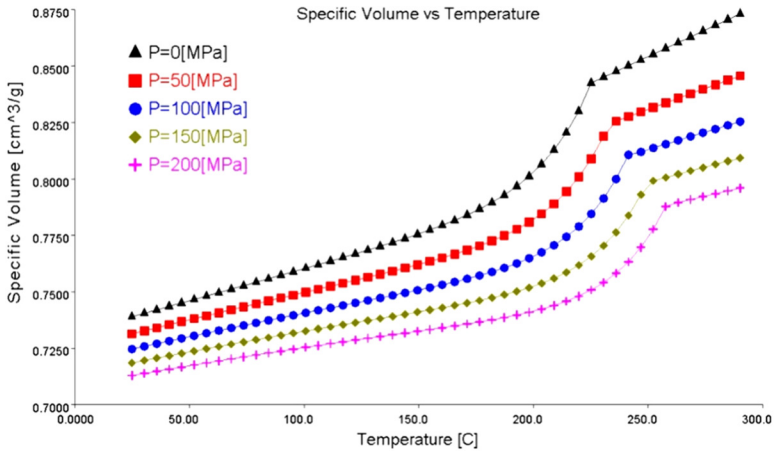

Fig. 2. pvT diagram for PBT/PET 15GF (Moldflow Materials Database)

The curves were determined using the Cross-WLF rheological model. It is a seven-parameter model frequently used in simulation software for the injection molding process.

For the visualization studies, a specialized injection mold with a unique design was used, as presented in detail by the author in publication [7]. This mold allowed the authors to record the phenomena occurring during the flow of the material inside the molding cavity. The mold was equipped with two viewing windows, each with a surface area at least equal to that of the cavity, made of crystalline glass commercially known as Zerodur® (Schott AG, Germany) [19]. This material is characterized by an almost zero thermal expansion coefficient, which makes it resistant to rapid temperature changes occurring during cavity filling.

The recording was carried out using a digital video camera. Additionally, a dedicated illumination setup based on LED diodes was installed to ensure proper visibility. The recordings were performed in complete darkness in a controlled laboratory environment.

Figure 3 presents the FEM model of the molded part. It was a rectangular prism-shaped part with three obstacles: a semicircle, a quarter-circle, and a triangle. Additionally, the mold's gating system was modeled.

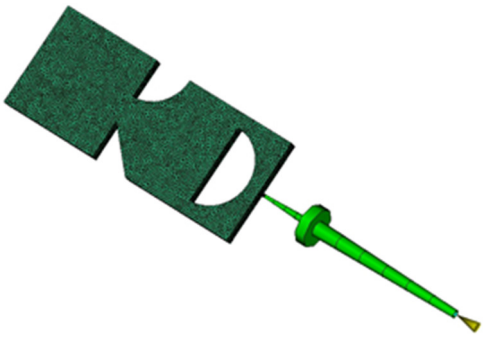

Fig. 3. Model of the molded part and the gating system with a superimposed finite element mesh

4. Research results

After entering the material data and processing conditions, appropriate numerical calculations were performed. Conducting simulations of selected phenomena required the use of a model that met specific criteria (the number of finite elements per wall thickness of the molded part could not be fewer than six).

Simultaneously, the flow of the material in the injection mold was recorded. A comparison of experimental and simulation results is presented in Figure 4. This comparison includes a juxtaposition of frame-by-frame images captured by a digital video camera with corresponding computer simulation results of the injection molding process. The presented comparison pertains to a process conducted under the following conditions:

- Volumetric flow rate: 30 cm^3/s
- Maximum injection pressure: 80 MPa
- Injection time: 2.5 s
- Cooling time: 30 s
- Injection temperature: 240 °C
- Mold temperature: approximately 25 °C.

Several phenomena previously described only in theoretical terms were recorded. The flow of molten material around various obstacles, the propagation of gas bubbles and other inclusions were documented, as well as the occurrence of streamwise flow, material runoff, and collisions of material streams. The research results presented in this study indicate that streams of plasticized composite exhibit properties characteristic of a viscoelastic material (as expected by the authors). Upon encountering an obstacle at high flow velocity, the material does not form a stream in the advancing direction but instead alters its trajectory precisely by flowing along the obstacle's surface. This confirms theoretical predictions and numerical analyses concerning the flow of viscoelastic materials (liquids).

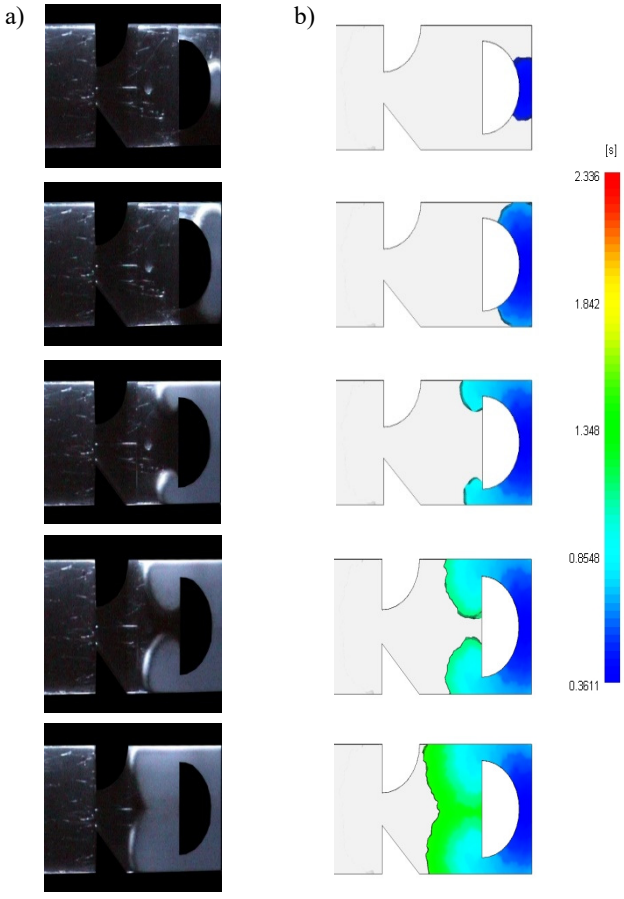

Fig. 4. Summary of experimental (a) and simulation results (b)

5. Conclusions

The comparison of polymer flow observations in the injection molding process with the results of simulations allows us to conclude that specialized computer software is capable of reliably predicting phenomena specific to polymer processing. Modern simulation programs offer a high degree of accuracy (assuming the correctness of the initial and boundary conditions and the reliability of the material data of the processed polymer). This means that already at the design stage, the manufacturing process can be anticipated and optimized. Until recently, not all flow-related phenomena could be numerically modeled. However, ongoing advancements in simulation software have now made it possible to model virtually all phenomena occurring during the filling of the injection mold cavity.

The material chosen for the research, besides its interesting rheological properties, also has an appropriate color in the plastic state (due to the conditions for recording the flow), which has significantly improved the quality of the results.

The search for new research methods aims to deepen knowledge of previously unexplained or debated phenomena occurring during selected manufacturing processes. Such studies seek to understand, analyze, and utilize these phenomena to optimize and minimize manufacturing costs.

The comparison of composite flow observations in the injection molding process with the results of simulation studies confirms that specialized computer software enables the prediction of phenomena specific to a given manufacturing process. This means that, already at the design stage, the manufacturing process can be anticipated and optimized.

Moreover, the construction of specialized research stations facilitates the in-depth examination of previously unconfirmed theoretical predictions concerning phenomena occurring during complex manufacturing processes.

References

[1] Yokoi, H., & Takematsu, S. (2002). Visualization of burning phenomena during cavity filling process. *PPS Guimaraes*. Conference Proceedings.

[2] Yang, S.Y., Nian, S.C., & Sun, I.C. (2002). Flow visualization of filling process during micro-injection molding. *International Polymer Processing*, *17*(4), 354-360.

[3] Hasegawa, S., Yokoi, H., & Murata, Y. (2003). Dynamic visualization of cavity filling process in ultra-high speed and thin wall injection molding. *PPS Athens*. Conference Proceedings.

[4] Banasiak, A., Błędzki, A., & Sterzyński, T. (2003). Flow lines visualization by injection molding of a model system PE + talc. *PPS Athens*. Conference Proceedings.

[5] Guerrier, P., Tosello, G., & Hattel, J.H. (2017). Flow visualization and simulation of the filling process during injection molding. *CIRP Journal of Manufacturing Science and Technology*, *16*, 12-20.

[6] Banasiak, A., & Sterzyński, T. (2004). Ocena przepływu w formie wtryskowej polimeru z napełniaczem płytkowym jako znacznikiem. *Polimery*, *49*(6), 442-448.

[7] Nabiałek, J. (2004). Prototyp formy do monitorowania i rejestracji przepływu tworzywa w procesie wtryskiwania. In: *Materiały polimerowe i ich przetwórstwo*. Praca zbiorowa, 325-331.

[8] Alves de Miranda, D., Rauber, W.K., Vaz, M., Canhoto Alves, M.V., Humel Lafratta, F., Lourenço Nogueira, A., & Berving Zdanski, P. (2023). Analysis of numerical modeling strategies to improve the accuracy of polymer injection molding simulations. *Journal of Non-Newtonian Fluid Mechanics*, *315*(1), 105033.

[9] Ji, K., Gao, R., Chen, H., Fu, J., & Zhao, P. (2024). Visualization and monitoring of the injection molding process using ultrasonic phased array. *Journal of Materials Processing Technology*, *326*, 118322.

[10] Guerrier, P., Tosello, G., & Hattel, J.H. (2014). Analysis of cavity pressure and warpage of polyoxymethylene thin walled injection molded parts: Experiments and simulations. Proceedings of the 30th International Conference of the Polymer Processing Society (PPS-30). Cleveland, 5 pages.

[11] Wilczyński, K. (2000). *Reologia w przetwórstwie tworzyw sztucznych*. WNT, Warszawa.

[12] Sangroniz, L., Fernandez, M., & Santamaria, A. (2023). Polymers and rheology: A tale of give and take. *Polymer*, *271*, 125811.

[13] Xu, X., & Yu, P. (2017). Modeling and simulation of injection molding process of polymer melt by a robust SPH method. *Applied Mathematical Modelling*, *48*, 384-409.

[14] Spina, R. (2017). Numerical-experimental investigation of PE/EVA foam injection molded parts. *Results in Physics*, *7*, 2775-2790.

[15] Glowinski, R., & Wachs, A. (2011). *On the numerical simulation of viscoplastic fluid flow*. In: R. Glowinski & J. Xu (Eds.), *Handbook of Numerical Analysis,* 16, 483-717. Elsevier.

[16] Dyi-Cheng, Ch., Rih-Sheng, Y., Shang-Wei, L., & Hong-Yao, G. (2022). Application of mold flow analysis to the study of plastic gear rack injection molding warpage. *Transactions of The Canadian Society for Mechanical Engineering, 47*(1), 15-25.

[17] Köhler, D., Gröger, B., Kupfer, R., Hornig, A., & Gude, M. (2020). Experimental and numerical studies on the deformation of the flexible wire in an injection moulding process. *Procedia Manufacturing*, *47*, 940-947.

[18] Wang, J., Hopmann, Ch., Schmitz, M., & Hohlweck, T. (2019). Modeling of pvT behavior of semi-crystalline polymer based on the two-domain Tait equation of state for injection molding. *Materials and Design*, *183*, 108149.

[19] http:/www.schott.com/lithotec.